Advances in Nano Research, *Vol. 10, No. 4 (2021) 385-395*
DOI: https://doi.org/10.12989/anr.2021.10.4.385

Geometrically nonlinear thermo-mechanical bending analysis of deep cylindrical composite panels reinforced by functionally graded CNTs

Sattar Jedari Salami [1a], Mostafa Sabzikar Boroujerdy [2b] and Ehsan Bazzaz*[3]

[1] *Department of Biomedical Engineering, Central Tehran Branch, Islamic Azad University, Tehran, Iran*
[2] *Department of Engineering, Firoozkooh Branch, Islamic Azad University, Firoozkooh, Iran*
[3] *Department of Mechanical Engineering, Central Tehran Branch, Islamic Azad University, Tehran, Iran*

(*Received January 24, 2020, Revised January 2, 2021, Accepted January 3, 2021*)

Abstract. This research concentrates on the effects of distributions and volume fractions of carbon nanotubes (CNT) on the nonlinear bending behavior of deep cylindrical panels reinforced by functionally graded carbon nanotubes under thermo-mechanical loading, hitherto not reported in the literature. Assuming the effects of shear deformation and moderately high value of the radius-to-side ratio (R/a), based on the first-order shear deformation theory (FSDT) and von Karman type of geometric nonlinearity, the governing system of equations is obtained. The analytical solution of field equations is carried out using the Ritz method together with the Newton-Raphson iterative scheme. The effects of radius-to-side ratio, temperature change, and boundary conditions on the nonlinear response of the functionally graded carbon nanotubes reinforced composite deep cylindrical panel (FG-CNTRC) are investigated. It is concluded that, among the five possible distribution patterns of CNT, FG-V CNTRC deep cylindrical panel is strongest with the highest bending moment and followed by UD, X, O, and Λ-ones. Also, considering the present deep cylindrical panel formulation increases the accuracy of the results. Hence, according to the noticeable amount of R/a in FG-CNTRC cylindrical panels, it is mandatory to apply strain-displacement relations of deep cylindrical panels for bending analysis of FG-CNTRC which certainly is desirable for industrial application.

Keywords: deep cylindrical panel; mechanical and thermal loading; functionally graded carbon nanotube composites

1. Introduction

Gradually distribution of carbon nanotubes (CNTs) in a polymeric or metallic matrix creates a new class of materials that are called functionally graded carbon nanotube reinforced composites (FG-CNTRC). Researches about this class of materials have grown rapidly in recent years. The main reason for this attention is related to special properties of FG-CNTRC such as high strength, high stiffness, and high aspect ratio, and very low density. Different researches about the mechanical analysis of FG-CNTRCs were reviewed by Liew *et al*. (2015).

There are lots of researches about CNTs in different fields like Chang and Gao (2003), Song and Youn (2006), Khater *et al*. (2015), Hajnayeb and Khadem (2015), Kumar and Sirvastava (2016), Karimov *et al*. (2020) and Navneeth *et al*. (2020). But the first work about the effect of FG-CNT on the behavior of the mechanical structure is done by Shen (2009). He studied nonlinear bending of a simply supported functionally graded reinforced composite plate under transverse loading. Also, the thermal effect is included by considering the material properties of the plate as a function of temperature. His results show that FG-CNT has a remarkable effect on the bending behavior of plates. Wang and Shen (2011) investigated the nonlinear vibration of FG-CNTRC plates using the perturbation technique. In their study, they used plates with an elastic foundation in a thermal environment. The results show a considerable effect of CNT volume fraction on vibration characteristics of plates such as natural frequency. The same authors (Wang and Shen 2012) carried out nonlinear vibration and bending of sandwich plates with FG-CNT face sheets on an elastic foundation. They used different kinds of CNT distribution in the thickness direction of sheets. The results for vibration and bending illustrate the high effect of CNT distribution and volume fraction on the linear and nonlinear behavior of plates. Lei *et al*. (2013) presented a free vibration analysis of FG-CNTRCs plates, using the element-free kp-Ritz method. The governing equations are based on the first-order shear deformation plate theory and the two-dimensional displacement fields are approximated by mesh-free kernel particle functions. For different volume fraction distributions, the results showed the effect of plate width-to-thickness ratio, plate aspect ratio, and temperature change on natural frequencies and mode shapes of various types of FG-CNTRC plates. Chavan and Lal (2017) considered the bending behavior of single-wall carbon nanotube reinforced functionally graded plates under sinusoidal transverse loading. They used the finite element method based on the higher-order shear deformation theory in their analysis. Their results show stress distribution and deflection of the plate under the different boundary conditions, carbon

*Corresponding author, Ph.D., Professor,
E-mail: sattar.salami@aut.ac.ir
[a] Ph.D.
[b] Ph.D.

ISSN: 2287-237X (Print), 2287-2388 (Online)

nanotube distribution, and geometrical ratios.

Using the size effect for the first time, Karami *et al*. (2018) presented a comprehensive study of Functionally Graded Carbon Nanotube Reinforced Composite plates based upon Second-Order Shear Deformation Theory (SSDT). They studied the effect of different parameters such as volume fraction of carbon nanotube, nonlocality, and elastic foundation on static, stability, and dynamic response of FG-CNTRC plates with Winkler–Pasternak elastic foundation. Kamarian *et al*. (2019) investigated the effect of CNTs on thermomechanical behavior of epoxy-based composite plates. They used experimental and numerical methods for their analysis. Results show that coefficient of thermal expansion has a decreasing-increasing trend according to the weight percentage of CNTs. Hajmohammad *et al*. (2018) analyzed buckling of piezoelectric FG-CNTRC truncated conical shells in a hygrothermal environment. A layerwise shear deformation theory was applied and the Halpin- Tsai model was used for obtaining the effective moisture and temperature-dependent material properties. The results illustrate that enhancing the CNTs' weight percent increases the buckling load. Furthermore, increasing the moisture and temperature changes decreases the buckling load. Kamarian *et al*. (2015, 2016) studied the effect of CNTs agglomeration on the vibrational behavior of FGS-CNTR beams. Their analysis based on the Timoshenko beam theory and GDQ method. The results show the serious effect of CNTs agglomeration on the mechanical and vibrational behavior of FGS-CNTR beams. Also, they considered the influence of foundation, piezoelectric layers thickness and geometrical parameters in their work.

Jedari Salami (2016a, b, 2017, 2018) presented a series of works related to sandwich panel beams with FG-CNTRC face sheets. In all of them, the governing equations are based on the Extended High Order Sandwich Panel Theory (EHSAPT). The first study is related to bending of the beams under line load at the top face sheet for different boundary conditions. The influence of the distribution pattern of CNTs on moment resultants, stress, and displacement of core and sheets of the sandwich beam using the Ritz method is reported in this study. The second study is related to the response of beams under low-velocity impacts. Again, the field equations are derived using the Ritz method and the contact force is calculated according to conventional Hertz law. Also, the time-domain solution is derived using the Runge-Kutta method. Results show the effect of different parameters such as CNTs distribution on the contact characteristics. In the last one, the transient response of sandwich beams under dynamic loading was investigated. The results are derived for different boundary conditions using the Ritz method and Newmark direct integration method. The results show the effect of nanotube volume fraction and their distribution on the time domain transverse displacement, shear force, and moment resultants of the face sheet. Based on Euler- Bernoulli beam theory, Hussain *et al*. (2019) studied the vibration analysis of armchair and zigzag single-walled carbon nanotubes. The Fourier method was utilized to solve the ordinary differential equation. The motion equation for this system was developed using a novel wave propagation method. The results were validated with existing open text.

Shen and Xiang (2014) studied the nonlinear bending of FG-CNT cylindrical shells on an elastic foundation and thermal environment. They used governing equations based on a higher-order shear deformation theory with a von Kármán-type of kinematic nonlinearity and solved them by a two-step perturbation technique. Ansari *et al*. (2014, 2015) studied forced vibration of FG-CNTRC beams and plates. Their governing equations for beams and plates are based on Timoshenko and the first-order shear deformation theories. They used generalized differential quadrature (GDQ) and Galerkin numerical methods for their analysis. The results show the CNT effects on nonlinear forced vibration characteristics of composite plates. Zhang *et al*. (2015a, b) researched the vibration characteristics of FG-CNTRC cylindrical panels, rectangular plates, and skew plates. The results are derived based on the first-order shear deformation theory (FSDT) and using Ritz Method. Effect of CNT on vibration frequencies and mode shapes are presented in the results. Using the GDQ method, Emdadi *et al*. (2019) studied the free vibration response of annular sandwich plates with various FG porous cores and FG-CNTRC face sheets based on modified couple stress theory and first-order shear deformation theories. The effects of material length scale parameters, boundary conditions, aspect and inner to outer radius ratios, FG porous distributions, pore compressibility, and volume fractions of CNTs were considered.

Mirzaei and Kiani (2015) investigated linear thermal buckling of FG-CNTRC conical shells by considering temperature-dependent materials. In their analysis, firstly equilibrium equations based on FSDT and Donnell equation are derived, and then for the stability equation, adjacent equilibrium criterion is applied. The pre-buckling load is derived using linear membrane analysis. The same authors (2016) studied the vibration characteristics of FG-CNTRC cylindrical panels for different kinds of boundary conditions. They used the same theories as to the previous one but the Ritz method with Chebyshev polynomials is used in the solution approach. The results illustrate that natural frequencies are proportional to the volume fraction of CNT.

Jamali *et al*. (2019) investigated CNTs' influence on postbuckling of the microplate with cut out subjected to a magnetic field and resting on elastic medium. The basic formulation of the plate is based on first-order shear deformation theory (FSDT) and the material properties of FG-CNTRCs are presumed to be changed through the thickness direction and are assumed based on the rule of mixture; moreover, nonlocal Eringen's theory was applied to consider the size-dependent effect. that the aspect ratio and length of square cut out have a negative effect on the postbuckling response of micro composite plate. Furthermore, the existence of CNTs in the system causes improvement in the postbuckling behavior of the plate and different distributions of CNTs in the plate have a diverse response. Ebrahimi and Habibi (2017) analyzed the nonlinear low-velocity impact response of FG-CNTRC plate based on the Eshelby- Mori- Tanaka approach in

thermal conditions using higher-order shear deformation plate theory (HSDT). The contact force between the impactor and laminated plate is obtained with the aid of the modified nonlinear Hertzian contact law models. In this research, the effect of layup and lamination angle as well as the effect of temperature variations, distribution of CNTs, the volume fraction of the CNTs, the mass and the velocity of the impactor in a constant energy level and boundary conditions on the impact response of the CNTRC laminated plates are investigated in details. Fu *et al*. (2019) analyzed the mechanical behavior of FG-CNTRC plates. They considered elastic foundations and thermal environment in their analysis. The equations are based on nth-order shear deformation theory and the differential quadrature method is used for the solution. Chan *et al*. (2019) investigated nonlinear buckling and post-buckling of FG-CNTRC truncated conical shells under the axial loading. The governing equations are based on classical shell theory and solved by Airy stress function and Galerkin method. Results show the effect of different parameters such as volume fraction, geometric ratios, and elastic foundations on the buckling and postbuckling behavior of the conical shell.

In this paper, nonlinear bending analysis of deep cylindrical composite panels reinforced by functionally graded carbon nanotubes (FG-CNT) is studied. Firstly, the equilibrium equations are derived using the total potential energy of the panel. Then using Ritz numerical method, the equilibrium equations are solved and the results are derived. Finally, the influence of nanotubes distributions and volume fraction, temperature changes, and boundary conditions on transverse displacement and moment resultants is investigated. Comparison of present work with other works shows a good agreement between the results. It should be noted that according to the noticeable amount of the radius-to-side ratio (R/a) in FG-CNTRC cylindrical panels, it is mandatory to apply strain-displacement relations of deep cylindrical panels for bending analysis of FG-CNTRC.

2. Governing formulation

Consider an FG-CNTRC panel with thickness h and mean radius R in reference coordinate XYZ as shown in Fig. 1 where the displacement components of the middle surface are u, v, and w along with the longitudinal, circumferential and lateral directions, respectively.

For this coordinate system, the kinematics equations of a deep cylindrical panel according to the first-order shear deformation theory could be written as (Asadi *et al*. 2012)

$$\begin{aligned}
\varepsilon_x &= u_{,x} + \frac{1}{2}w_{,x}^2 + z\phi_{x,x} - \alpha_{11}\Delta T \\
\varepsilon_y &= v_{,y} + \frac{w}{R} + \frac{1}{2}\left(w_{,y}{}^2 + \left(\frac{v}{R}\right)^2\right) \\
&\quad + z\left(\phi_{y,y} + \frac{v_{,y}}{R}\right) - \alpha_{22}\Delta T \\
\gamma_{xy} &= v_{,x} + u_{,y} + w_{,x}\left(w_{,y} + \frac{v}{R}\right) \\
&\quad + z\left(\phi_{x,y} + \phi_{y,x} + \frac{v_{,x}}{R}\right) \\
\gamma_{xz} &= \phi_x + w_{,x} \\
\gamma_{yz} &= \phi_y + w_{,y} - \frac{v}{R}
\end{aligned} \tag{1}$$

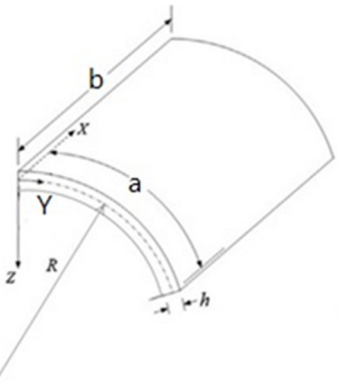

Fig. 1 The geometry of the cylindrical panel

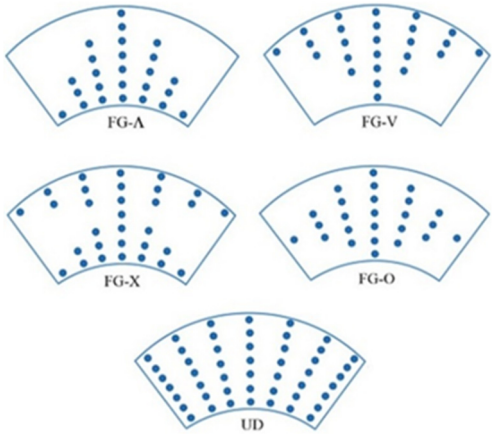

Fig. 2 Different distributions of nanotubes in cylindrical panels

Where in these equations, ϕ_x and ϕ_y are the rotations about circumferential and longitudinal coordinate's axes respectively. FG-CNTRC structures represent different behavior according to various types of CNTs distributions. In this paper, five different kinds of distribution for carbon nanotubes in the matrix of the cylindrical panel is considered. These different distributions are uniform distribution (UD), and four graded distribution: FG-V, FG-Λ, FG-O, and FG-X as shown in Fig. 2.

For different kinds of CNT distribution, the volume fraction mathematical equations are

$$V_{CN}(z) = \begin{cases} V_{CN}^* & (UD\ CNTRC) \\ 2V_{CN}^*\left(1 - 2\dfrac{|z|}{h}\right) & (FG-O\ CNTRC) \\ 4V_{CN}^*\dfrac{|z|}{h} & (FG-X\ CNTRC) \\ V_{CN}^*\left(1 + 2\dfrac{z}{h}\right) & (FG-V\ CNTRC) \\ V_{CN}^*\left(1 - 2\dfrac{z}{h}\right) & (FG-\Lambda\ CNTRC) \end{cases} \tag{2}$$

Where $-\frac{h}{2} \le z \le \frac{h}{2}$. In this equation V_{CN} and V_{CN}^* present CNT volume fraction of each distribution and total volume fraction, respectively. From Eq. (2) it can be concluded that despite different CNT volume fractions, the

total volume fraction of CNT for different distributions are the same. The value of the total CNT volume fraction, V_{CN}^{*}, is derived by (Shen 2009)

$$V_{CN}^{*}=\frac{\mathrm{w_{CN}}}{\mathrm{w_{CN}}+(\rho^{\mathrm{CN}}/\rho^{\mathrm{m}})-(\rho^{\mathrm{CN}}/\rho^{\mathrm{m}})\,\mathrm{w_{CN}}} \tag{3}$$

Where ρ^{m}, ρ^{CN} and w_{CN} are matrix density, CNT density, and mass fraction of CNT, respectively. Using matrix and carbon nanotubes properties, the mechanical properties of the reinforced panel are calculated according to the conventional rule of the mixture as (Shen 2009)

$$\begin{aligned}
&\mathrm{E_{11}}=\eta_1\mathrm{V_{CN}}\mathrm{E_{11}^{CN}}+\mathrm{V_m}\mathrm{E^m}\\
&\frac{\eta_2}{\mathrm{E_{22}}}=\frac{\mathrm{V_{CN}}}{\mathrm{E_{22}^{CN}}}+\frac{\mathrm{V_m}}{\mathrm{E^m}}\\
&\frac{\eta_3}{\mathrm{G_{12}}}=\frac{\mathrm{V_{CN}}}{\mathrm{G_{12}^{CN}}}+\frac{\mathrm{V_m}}{\mathrm{G^m}}
\end{aligned} \tag{4}$$

V_{CN} and V_m are volume fraction of CNTs and matrix, respectively, which are related as

$$V_{CN}+V_m=1 \tag{5}$$

$\mathrm{E_{11}^{CN}}$, $\mathrm{E_{11}^{CN}}$ and $\mathrm{E_{11}^{CN}}$ present Young's modulus and shear modulus of carbon nanotubes. Also E^m and G^m are corresponding mechanical properties of the matrix as an isotropic and homogeneous material. Parameters η_i (i = 1, 2, 3) are the so-called efficiency parameters that are used for size-dependent properties to compensate for the difference in the result of the conventional rule of mixture. The Poisson's ratio of the panel is considered almost independent of CNTs distribution (Shen 2009) and is related to Poisson's ratio of CNT, ν_{12}^{CN}, and Poisson's ratio of the matrix, ν^m, by

$$\nu_{12}=\mathrm{V}_{CN}^{*}\nu_{12}^{\mathrm{CN}}+\mathrm{V_m}\nu^m \tag{6}$$

Finally, thermal expansion coefficients of FG-CNTRC cylindrical panel according to Sharpy model in longitudinal and circumferential directions are (Shen, 2012)

$$\begin{aligned}
&\alpha_{11}=\frac{V_{CN}E_{11}^{CN}\alpha_{11}^{CN}+V_mE^m\alpha^m}{V_{CN}E_{11}^{CN}+V_mE^m}\\
&\alpha_{22}=(1+\upsilon_{12}^{CN})V_{CN}\alpha_{22}^{CN}+(1+\upsilon^m)V_m\alpha^m-\upsilon_{12}\alpha_{11}
\end{aligned} \tag{7}$$

α_{11}^{CN}, α_{22}^{CN} are thermal expansion coefficients of CNT, α^m is thermal expansion coefficients of the matrix, υ_{12}^{CN} is Poisson's ratio of CNT and υ^m is Poisson's ratio of the matrix. According to the plane stress form of Hook's law and mentioned relations, the stress-strain relations of FG-CNTRC panel could be written as

$$\begin{aligned}
&\sigma_{\mathrm{x}}=Q_{11}\varepsilon_x+Q_{12}\varepsilon_y\\
&\sigma_{\mathrm{y}}=Q_{12}\varepsilon_x+Q_{22}\varepsilon_y\\
&\tau_{\mathrm{yz}}=Q_{44}\gamma_{yz}\\
&\tau_{\mathrm{xz}}=Q_{55}\gamma_{xz}\\
&\tau_{\mathrm{xy}}=Q_{66}\gamma_{xy}
\end{aligned} \tag{8}$$

where Q_{ij} are components of the stiffness matrix of a cylindrical panel that compatible with plane stress conditions. These coefficients are calculated by

$$\begin{aligned}
&\mathrm{Q_{11}}=\frac{\mathrm{E_{11}}}{1-\nu_{12}\nu_{21}}\\
&\mathrm{Q_{22}}=\frac{\mathrm{E_{22}}}{1-\nu_{12}\nu_{21}}\\
&\mathrm{Q_{12}}=\frac{\nu_{21}\mathrm{E_{11}}}{1-\nu_{12}\nu_{21}}\\
&Q_{44}=G_{23}\qquad Q_{55}=G_{13}\qquad Q_{66}=G_{12}
\end{aligned} \tag{9}$$

3. Method of solution

For starting the solution of the problem, using the Ritz method, the equilibrium equations of the panel must be derived. The total potential energy of panel (Π) is obtained by summation of strain energy (U) and potential energy of external forces (W)

$$\Pi=\mathrm{U}+\mathrm{W} \tag{10}$$

The strain energy of the panel is calculated as

$$\begin{aligned}
U=\int\Big(&\frac{1}{2}\varepsilon_x\sigma_x+\frac{1}{2}\varepsilon_y\sigma_y+\frac{1}{2}\tau_{yz}\gamma_{yz}+\frac{k}{2}\tau_{xz}\gamma_{xz}\\
&+\frac{\mathrm{k}}{2}\tau_{xy}\gamma_{xy}\Big)dV
\end{aligned} \tag{11}$$

Where k is the shear correction factor that depends on different parameters such as boundary conditions and geometrical characteristics. In this paper, the value of k is approximated as $\frac{5}{6}$. Substituting Eq. (8) into Eq. (11) yields

$$\begin{aligned}
U=\int\Big(&\frac{1}{2}Q_{11}\varepsilon_x^2+\frac{1}{2}Q_{22}\varepsilon_y^2+Q_{12}\varepsilon_x\varepsilon_y+\frac{\mathrm{k}}{2}Q_{44}\gamma_{yz}^2\\
&+\frac{\mathrm{k}}{2}Q_{55}\gamma_{xz}^2+\frac{1}{2}Q_{66}\gamma_{xy}^2\Big)dV
\end{aligned} \tag{12}$$

Also, the potential energy of external forces is

$$W=\int -Pw\,dA \tag{13}$$

P and w, are external loads and lateral displacement, respectively. By substitution of Eqs. (12) and (13) in Eq. (10), the total potential energy of the panel is derived as

$$\Pi=\int\left(\frac{1}{2}Q_{11}\varepsilon_x^2+\frac{1}{2}Q_{22}\varepsilon_y^2+Q_{12}\varepsilon_x\varepsilon_y+\frac{\mathrm{k}}{2}Q_{44}\gamma_{yz}^2\right) \tag{14}$$

Finally, substituting Eq. (1) in Eq. (14) yields

$$\begin{aligned}
\Pi=\int\Big[&\frac{1}{2}Q_{11}\Big(u_{,x}+\frac{1}{2}w_{,x}^2+z\phi_{x,x}-\alpha_{11}\Delta T\Big)^2\\
&+\frac{1}{2}Q_{22}\Big(v_{,y}+\frac{1}{2}\Big({w_{,y}}^2+\Big(\frac{v}{R}\Big)^2\Big)\\
&+z\Big(\phi_{y,y}+\frac{v_{,y}}{R}\Big)\frac{w}{R}-\alpha_{22}\Delta T\Big)^2
\end{aligned} \tag{15}$$

$$+Q_{12}\left(u_{,x}+\frac{1}{2}w_{,x}^2+z\phi_{x,x}-\alpha_{11}\Delta T\right)\left(v_{,y}+\frac{w}{R}+\frac{1}{2}\left(w_{,y}{}^2+\left(\frac{v}{R}\right)^2\right)+z\left(\phi_{y,y}+\frac{v_{,y}}{R}\right)-\alpha_{22}\Delta T\right)+\frac{\mathrm{k}}{2}Q_{44}\left(\phi_y+w_{,y}-\frac{v}{R}\right)^2+\frac{\mathrm{k}}{2}Q_{55}\left(\phi_x+w_{,x}\right)^2+\frac{1}{2}Q_{66}\left(v_{,x}+u_{,y}+w_{,x}\left(w_{,y}+\frac{v}{R}\right)+z\left(\phi_{x,y}+\phi_{y,x}+\frac{v_{,x}}{R}\right)\right)^2\Bigg]dV-\int PwdA \quad (15)$$

Using the Ritz method for the discretization of Eq. (15) in the displacement domain, the following series are considered as approximated functions for displacements and rotations (Mirzae and Kiani 2015)

$$\begin{aligned}u&=R^u(x,y)\sum_{i=1}^{N_x}\sum_{j=1}^{N_y}U_{ij}P_i(x)P_j(y)\\ v&=R^v(x,y)\sum_{i=1}^{N_x}\sum_{j=1}^{N_y}V_{ij}P_i(x)P_j(y)\\ w&=R^w(x,y)\sum_{i=1}^{N_x}\sum_{j=1}^{N_y}W_{ij}P_i(x)P_j(y)\\ \phi_x&=R^x(x,y)\sum_{i=1}^{N_x}\sum_{j=1}^{N_y}X_{ij}P_i(x)P_j(y)\\ \phi_y&=R^y(x,y)\sum_{i=1}^{N_x}\sum_{j=1}^{N_y}\mathrm{Y}_{ij}P_i(x)P_j(y)\end{aligned} \quad (16)$$

The above equations are optional and only must satisfy the essential boundary conditions. $P_i(x)$ and $P_j(y)$ are *i-th* and *j-th* Chebyshev polynomial of the first kind that is defined as

$$\begin{aligned}P_i(x)&=\cos\left((i-1)\,arccos\left(\frac{2x}{a}\right)\right)\\ P_j(y)&=\cos\left((j-1)\arccos\left(\frac{2y}{b}\right)\right)\end{aligned} \quad (17)$$

where $-\frac{b}{2}\le x\le\frac{b}{2}$,- $\frac{a}{2}\le y\le\frac{a}{2}$ and N_x and N_y are a number of divisions in x and y-directions, respectively. R functions are boundary functions related to essential boundary conditions. Considering the origin of coordinate in the center of the panel's midplane, the R function could be selected as (Abrate 1998)

$$R(x.y)=\left(1+\frac{2x}{a}\right)^p\left(1-\frac{2x}{a}\right)^q\left(1+\frac{2y}{b}\right)^r\left(1+\frac{2\mathrm{y}}{b}\right)^s \quad (18)$$

where p, q, r, and s are equated to 0 or 1, according to the essential boundary conditions. In this paper two kinds of boundary conditions, movable and immovable simply supported boundary conditions, are considered. For movable simply supported boundary conditions, the essential boundary conditions are

$$\begin{aligned}w=\phi_y=0 \qquad x=-\frac{b}{2},\ \frac{b}{2}\\ w=\phi_x=0 \qquad y=-\frac{a}{2},\ \frac{a}{2}\end{aligned} \quad (19)$$

And for the immovable one, the essential boundary conditions could be written as

$$\begin{aligned}u=w=\phi_y=0 \qquad x=\frac{b}{2},\ \frac{b}{2}\\ v=w=\phi_x=0 \qquad y=-\frac{a}{2},\ \frac{a}{2}\end{aligned} \quad (20)$$

U, V, and W are unknown Coefficients that must be calculated. For this purpose, Eq. (15) is substituted in the Lagrange equation (Song and Youn 2006) as

$$\frac{\partial\Pi}{\partial s_{ij}^k}=0,\quad k=u,v,w,\quad i=1{:}\,N_x,\quad j=1{:}\,N_y \quad (21)$$

Where in this equation, $s_{ij}^u=U_{ij}$, $s_{ij}^v=V_{ij}$, $s_{ij}^w=W_{ij}$, $s_{ij}^x=X_{ij}$ and $s_{ij}^y=Y_{ij}$. Eq. (21) in matrix form could be written as

$$[K]\{S\}-\{F\}=\{R\}=0 \quad (22)$$

In this equation, $[K]$ is the coefficient matrix. Also, $\{S\}$ and $\{F\}$ are unknown and force vectors, respectively. Finally, $\{R\}$ is the residual vector that generally isn't zero and for deriving the results must be equated to zero. So, 5 $\times N_x \times N_y$ nonlinear equations are obtained. For the derivation of unknown components of the vector $\{S\}$ (*U*, *V*, *W*, *X*, and Y), Newton-Raphson method is implemented. In this method, a primary guess is considered for $\{S\}$ and then using iteration method, the other values of $\{S\}$ are obtained by

$$\{S\}_{n+1}=\{S\}_n-[\mathrm{K}_T]_n^{-1}\{R\}_n \quad (23)$$

Where n shows the number of iterations and $[K_T]$ is the tangential matrix that is obtained by

$$[K_T]=\frac{\partial R}{\partial s_{ij}^k} \quad (24)$$

its components are given in the Appendix. The iteration procedure is continuing till the difference between two consecutives $\{S\}$ is small sufficiently.

4. Results and discussion

In this section, the numerical results of the solution are presented. The results are derived for a cylindrical panel with thickness *h*, radius *R*, circumferential and longitudinal dimensions *a* and *b*, respectively. The material properties of the Polymethyl methacrylate, PMMA as the matrix are considered (Shen and Xiang 2014)

$$\begin{aligned}\mathrm{E}^{\mathrm{m}}&=(3.52-.0034T)\ \mathrm{GPa}\\ \alpha^{\mathrm{m}}&=45(1+0.0005\Delta T)\times\frac{10^{-6}}{K}\\ \upsilon^m&=0.34\end{aligned} \quad (25)$$

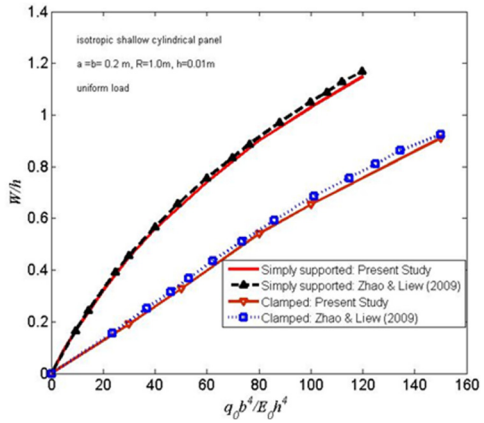

Fig. 3 Comparisons of load-deflection curves for an isotropic shallow cylindrical panel subjected to a uniform pressure

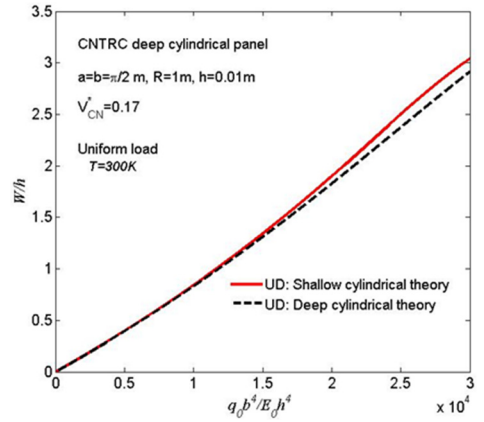

Fig. 4 Comparisons of load-deflection curves for an isotropic deep cylindrical panel based on shallow and deep cylindrical theories

In this equation $T = T_0 + \Delta T$ and $T_0 = 300\,K$. The thermomechanical properties of carbon nanotubes in the temperature range 300 to $700\,K$ are considered as (Mirzae and Kiani 2015)

Table 1 Maximum difference percentage of W/h from geometrical and present formulation viewpoints

	Deep cylindrical formulation (Fig. 3)		Geometrical aspect (Fig. 4)	
Shell type	Deep	Shallow	Deep	Shallow
w/h	0.88	0.85	3.05	2.88
Difference (%)	3.52%		6%	

$$
\begin{aligned}
E_{11}^{CN} &= (6.3998 - 4.338417 \times 10^{-3}\mathrm{T} \\
&\quad + 7.43 \times 10^{-6}\mathrm{T}^2 \\
&\quad - 4.45833 \times 10^{-9}\mathrm{T}^3)\ \mathrm{TPa} \\
E_{22}^{CN} &= (8.02155 - 5.420375 \times 10^{-3}\mathrm{T} \\
&\quad + 9.275 \times 10^{-6}\mathrm{T}^2 \\
&\quad - 5.5625 \times 10^{-9}\mathrm{T}^3)\ \mathrm{TPa} \\
G_{12}^{CN} &= (1.40755 + 3.476208 \times 10^{-3}\mathrm{T} \\
&\quad - 6.965 \times 10^{-6}\mathrm{T}^2 \\
&\quad + 4.479167 \times 10^{-9}\mathrm{T}^3)\ \mathrm{TPa} \\
\alpha_{11}^{CN} &= (-1.12515 + 0.02291688\mathrm{T} \\
&\quad - 2.887 \times 10^{-5}\mathrm{T}^2 \\
&\quad + 1.13625 \times 10^{-8}\mathrm{T}^3) \times \frac{10^{-6}}{K} \\
\alpha_{22}^{CN} &= (5.43715 - 0.984625 \times 10^{-4}\mathrm{T} \\
&\quad + 2.9 \times 10^{-7}\mathrm{T}^2 + 1.25 \times 10^{-11}\mathrm{T}^3) \\
&\quad \times \frac{10^{-6}}{K} \\
\nu_{12}^{CN} &= 0.175
\end{aligned}
\tag{26}
$$

And about the shear modulus, it is considered that (Shen 2009)

$$G_{12} = G_{13}, \qquad G_{23} = 1.2G_{12} \tag{27}$$

4.1 Comparison study

As part of the verification of the present study, the load-deflection curves for an isotropic cylindrical panel subjected to a uniform pressure are compared from three viewpoints. At first, to validate the assumption of considering strain-displacement of a deep cylindrical panel

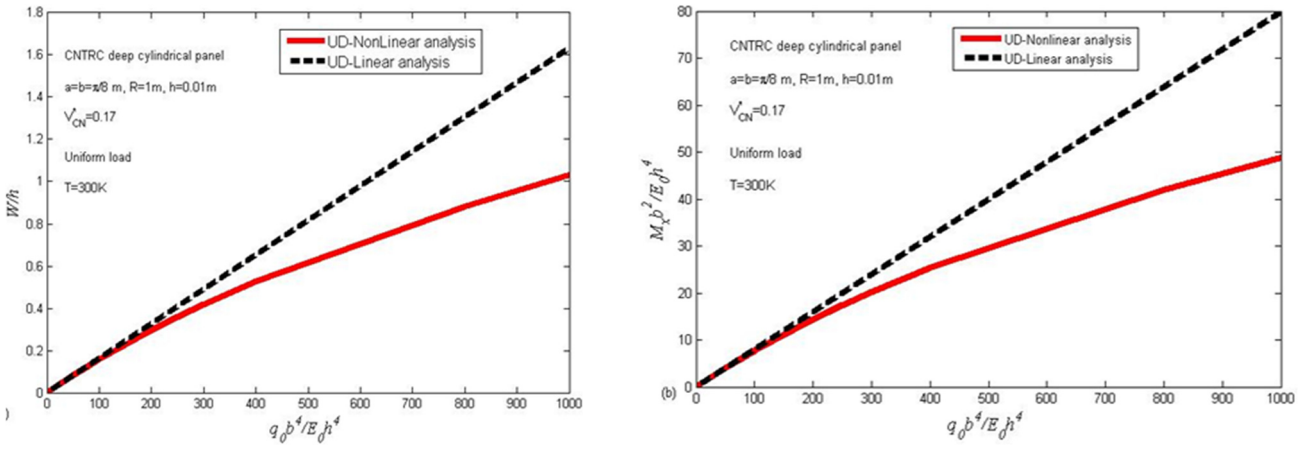

Fig. 5 (a) Comparisons of load-deflection behavior of CNTRC deep cylindrical panels based on geometrically linear and nonlinear analyses; (b) Comparisons of load-bending behavior of CNTRC deep cylindrical panels based on geometrically linear and nonlinear analyses

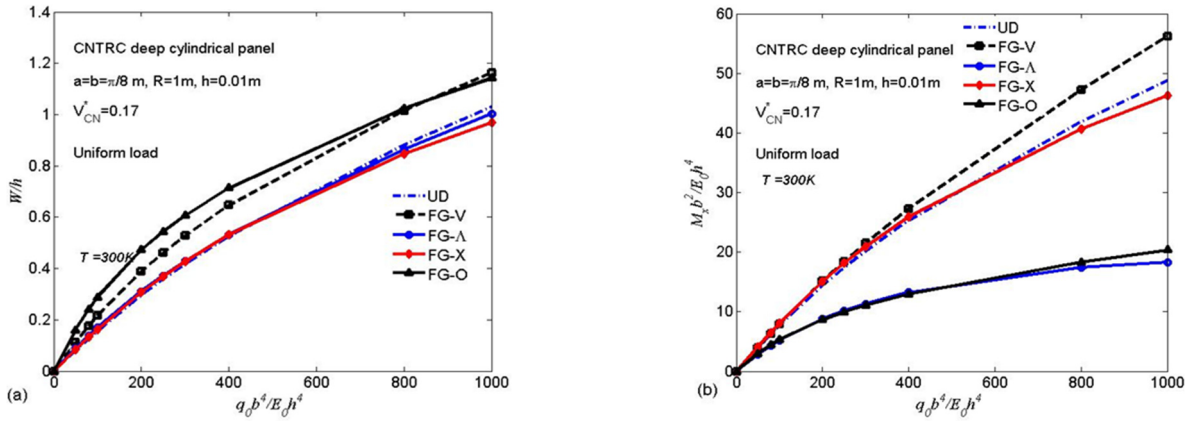

(a) Load-deflection (b) Load-bending moment

Fig. 6 Nonlinear bending behavior of CNTRC deep cylindrical panels with different types of CNT reinforcements

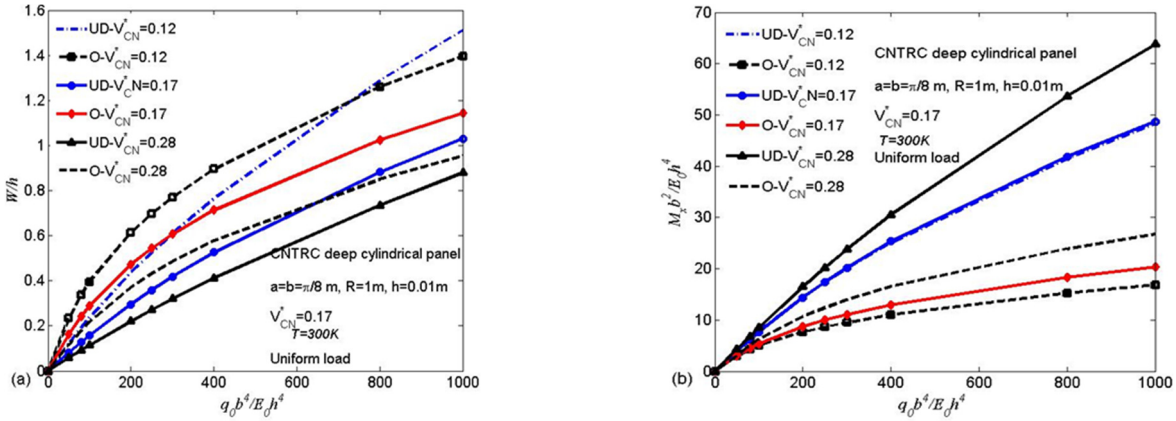

(a) Load-deflection (b) Load-bending moment

Fig. 7 Effect of nanotube volume fraction on the nonlinear bending behavior of CNTRC deep cylindrical panels

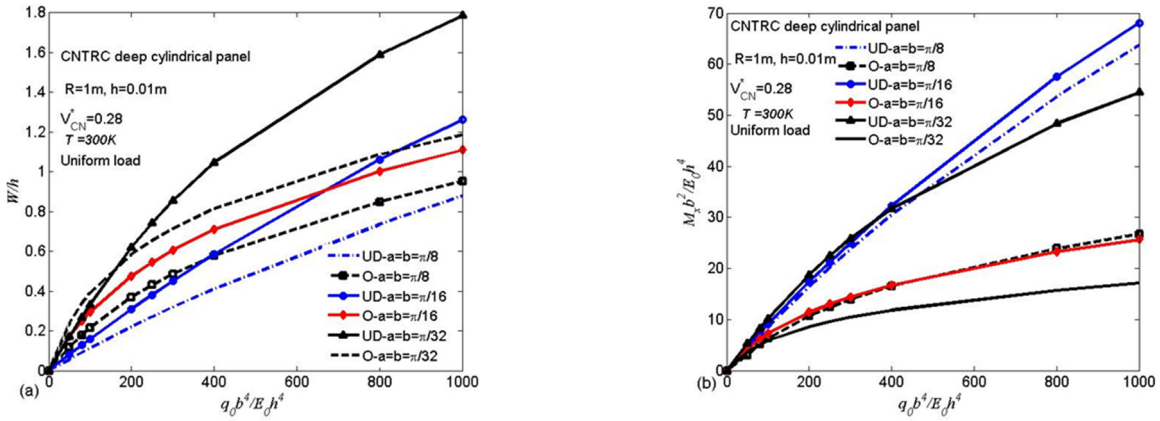

(a) Load-deflection (b) Load-bending moment

Fig. 8 Effect of radius-to-side ratio (R/a) on the nonlinear bending behavior of CNTRC deep cylindrical panels

to analyze shallow cylindrical panels, results are compared with those obtained by Zhao and Liew (2009), (see Fig. 3). In this case, the isotropic shallow cylindrical panel with radius-to- side ratio $\frac{R}{a} = 10$ and equal circumferential and axial edges are analyzed. As seen, there are very good agreements between the results. Second, comparison of results for the isotropic deep cylindrical panel with $\frac{R}{a} = \frac{\pi}{2} \cong 0.64$ based on shallow and deep cylindrical panel theories are depicted in Fig. 4. It may be concluded that the shallow cylindrical panel theory overestimates the central deflection of the deep panel. So, applying shallow theory encounter with unreal results in deep cylindrical panels. Table 1

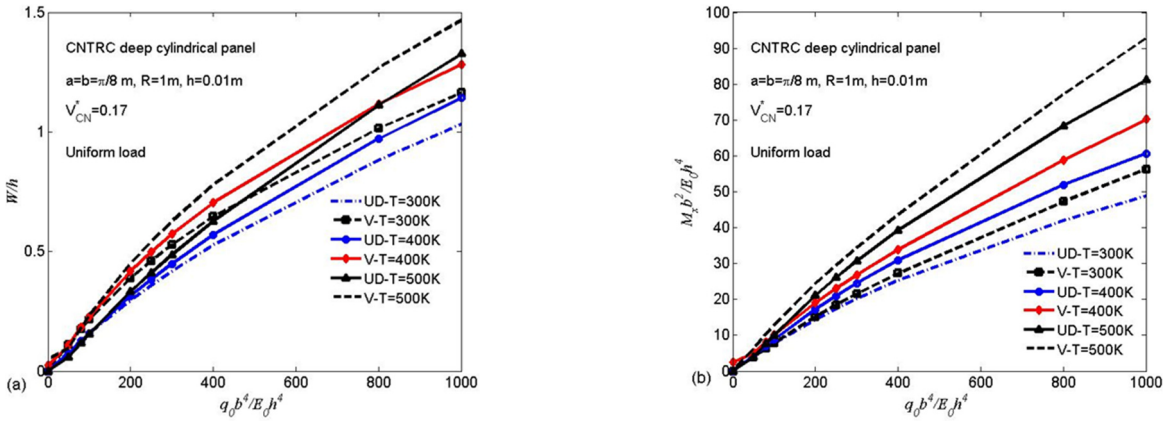

(a) Load-deflection (b) Load-bending moment

Fig. 9 The effect of temperature change on the nonlinear bending behavior of CNTRC deep cylindrical panels

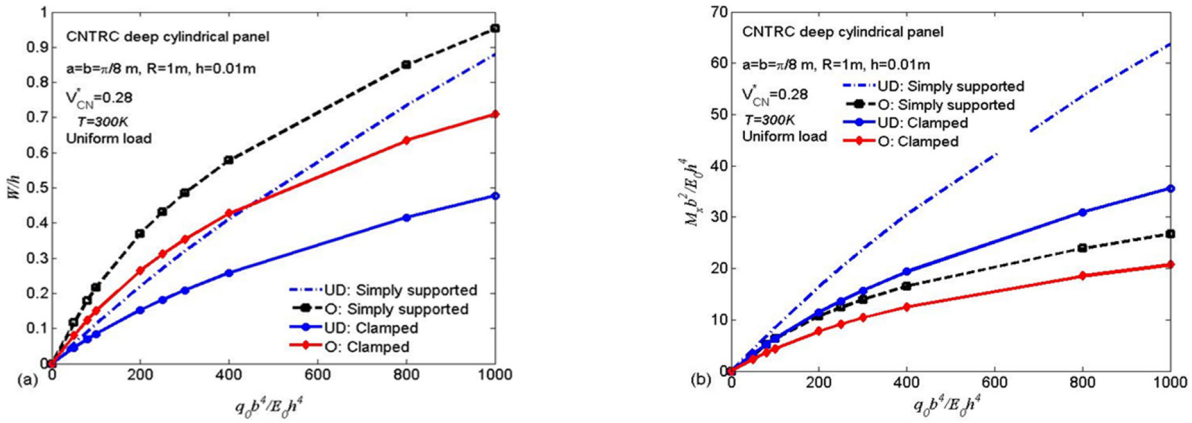

(a) Load-deflection (b) Load-bending moment

Fig. 10 Effect of type of boundary conditions on the nonlinear bending of CNTRC deep cylindrical panels

Table 2 Convergence study of the dimensionless central deflection (W/h) of the UD- CNTRC deep cylindrical panel with $V_{CN}^{*} = 0.17$ and $\frac{q_0 b^4}{E_0 h^4} = 1000$

Type of boundary condition	Number of terms (M)	Dimensionless central deflection (W/h)	Type of boundary condition	Number of terms (M)	Dimensionless central deflection (W/h)
Simply supported	1	0.6541	Immovable clamped	1	0.2578
	3	0.7984		3	0.3894
	5	0.8562		5	0.4527
	7	0.8756		7	0.4737
	9	0.8787		8	0.4774

demonstrates the maximum differences of dimensionless central deflection of the cylindrical panel according to the above-mentioned viewpoints. As seen, considering deep cylindrical formulation for cylindrical panels with a high radius- to- side ratio is mandatory. Also, it appears that deep cylindrical formulation can give good results for shallow cylindrical panels. Finally, to study the effects of nonlinear strain terms comparisons of results based on geometrically linear and nonlinear analyses are shown in Fig. 5. As seen, linear assumption predicts overestimate deflection and bending moment for $W/h > 0.1$ because the lower stiffness matrix is composed in linear analysis in comparison with that obtained from nonlinear one.

4.2 Parametric study

Numerical results are presented in this section for CNTRC deep cylindrical panels exposed to elevated temperature and subjected to a transverse uniform load in Figs. 6-10. For these examples, the deep panel has h = 0.01 m, axial and circumferential edges are equal and assumed to be $a = b = \frac{\pi}{8}$ except for the cases in Fig. 8. Four types of

FG-CNTRC deep cylindrical panels, i.e., FG-V, FG-X, FG-Λ, and FG-O are assumed as basic geometries. A UD-CNTRC cylindrical panel with the same geometric dimensions, referred to as UD, is also considered as a comparator. It should be noted that in all of the results $\frac{w}{h}$, $\frac{M_x b^2}{E_0 h^4}$ and $\frac{q_0 b^4}{E_0 h^4}$ illustrate the dimensionless central deflection of the deep panel, central bending moment, and transverse uniform load, respectively, in which E_0 Young's modulus of E_m at T = 300 K. The boundary conditions of the deep panels are considered to be simply supported, except for the cases in Fig. 10.

To assure the convergence of the series functions convergence studies are performed on the dimensionless central deflection of the UD-CNTRC deep cylindrical panel. Convergences of the dimensionless central deflection for two types of boundary conditions are listed in Table 2. Convergence is obtained when the difference between the results is in the order of 0.01. As seen in Table 2 the results are converged when the N_x and N_y equal to 9 and 7 for simply supported and immovable clamped boundary conditions, respectively.

The load-deflection and load- bending moment curves of the four types of FG-CNTRC deep panels and the UD-CNTRC deep panel subjected to transversely uniform load at T = 300 K are presented in Fig. 6. The CNT volume fraction is assumed to be V_{CN}^{*} = 0.17. It is observed that the deflection curves of FG-X, FG-Λ, and UD deep panels are similar and have significantly smaller deflections than the FG-O and FG-V deep panels. It is because with increasing CNT intensity in the lower surface of the panel, the stiffness of the lower surface increases and the central deflection decreases.

Also, it could be concluded that with increasing the stiffness of the lower layer, the bending moment of the deep panel is increased.

Fig. 7 illustrates the effect of CNT volume fraction on the nonlinear bending behavior of UD and FG-O CNTRC deep panels at T = 300 K. As seen the load-deflection curves are decreased, but the load-bending moment curves are increased when the CNT volume fraction V_{CN}^{*} is increased from 0.12 to 0.28 for both UD and FG-O CNTRC deep panels. It is because that the stiffness of CNTRC deep cylindrical panels is larger when the proportion of CNTs by volume is higher. The larger stiffness is obtained due to higher V_{CN}^{*} and causes lower central deflection with a higher bending moment.

Fig. 8 presents the effect of the radius –to- side ratio (R/a) on the nonlinear bending behavior of UD and FG-O CNTRC panels subjected to uniform load at T = 300 K. The panels are studied in the same radius (R = 1) with various side dimensions so that by increasing the R/a, the effect of depth of the panel is more noticeable. The results show that the CNTRC panels with higher R/a will undergo less deflection and have larger bending moments regardless of the type of CNT distribution. It is because by increasing the R/a while the R is kept constant, the length of the side arc is increased. So, the geometrical nonlinearity is increased with higher R/a and causes higher geometrical stiffness of the deep panel. Due to the increasing of geometrical stiffness with increasing the R/a, the lower deflections and higher bending moments are observed.

Fig. 9 shows the effect of temperature rise on the nonlinear bending behavior of UD and FG-V CNTRC deep panels. The CNT volume fraction is taken to be V_{CN}^{*} = 0.17 Three sets of thermal environmental conditions are assumed, i.e., T = 300, 400, and 500 K. It can be seen that the deflections are increased, but the bending moments are decreased by increasing in temperature for both UD and FG-V CNTRC deep panels.

It is because, with an increase in temperature, the stiffness of the panel is decreased and causes higher deflection and lower bending moment. The reason for that is increasing the temperature causes the softening of the panel. So, temperature increasing leads higher deflection and lower bending moment.

The effect of the geometrical boundary conditions on the nonlinear bending behavior of UD and FG-O CNTRC deep panels subjected at T = 300 K is presented in Fig. 10. The deep panel has $a = b = \pi/8$ m and R = 1 m. The CNT volume fraction is taken to be V_{CN}^{*} = 0.28. The results illustrate that the CNTRC deep panels with clamped edges undergo less deflection and higher bending moments. It is because clamped edges impose more constraints against deflection and cause higher geometrical stiffness of the panel. In other words, such a trend is interpreted based on the higher local flexural rigidity of the immovable clamped edge in comparison to a simply supported type.

5. Conclusions

Present research deals with the nonlinear bending analysis of deep cylindrical panels made of carbon nanotube-reinforced composite materials. The distribution of CNT across the panel thickness may be uniform or functionally graded. Properties of the composite media are obtained according to a refined rule of mixtures approach with the introduction of efficiency parameters into the rule of mixtures approach. First-order shear deformation shell theory and von Karman type of kinematic assumptions are used as the basic assumptions. A Ritz solution method in which with Chebyshev basis polynomials is developed to obtain accurate estimation of deflections as well as bending moments of the carbon nanotube reinforced deep panels with arbitrary edge supports. Parametric studies are conducted and numerical results are given as graphical presentations. Numerical results reveal that radius-to-side ratio (R/a) of the CNTRC deep cylindrical panel, volume fraction, a distribution profile of CNT, temperature rise, and boundary conditions are influential parameters on the nonlinear bending response of the deep panel. Increasing the R/a and volume fraction of CNT improves the geometrical and material stiffness of the deep cylindrical panel, respectively, and cause fewer deflections and higher bending moments. Furthermore, among the five possible distribution patterns of CNT, FG-V CNTRC deep cylindrical panel is strongest with the highest bending moment and followed by UD, X, O, and Λ-ones. On the other hand, it may be concluded that the present deep

cylindrical panel formulation capable to predict the accurate bending results of FG-CNTRC cylindrical panels. Therefore, according to the considerable influence of *R/a* in FG-CNTRC cylindrical panels, it is necessary to impose strain- displacement relations of deep cylindrical panels in bending analysis of them.

Acknowledgments

The research described in this paper was financially supported by the Central Tehran branch of Islamic Azad University.

References

Abrate, S. (1998), *Impact on Composite Structures*, Cambridge University Press, New York, NY, USA.

Ansari, R., Faghih Shojaei, M., Mohammadi, V., Gholami, R. and Sadeghi, F. (2014), "Nonlinear forced vibration analysis of functionally graded carbon nanotube-reinforced composite Timoshenko beams", *Compos. Struct.*, **113**, 316-327. https://doi.org/10.1016/j.compstruct.2014.03.015

Ansari, R., Hasrati, E., Faghih Shojaei, M., Gholami, R. and Shahabodini, A. (2015), "Forced vibration analysis of functionally graded carbon nanotube-reinforced composite plates using a numerical strategy", *Phys. E: Low. Dimens. Syst. Nanostruct.*, **69**, 294-305. https://doi.org/10.1016/j.physe.2015.01.011

Asadi, E., Wang, W. and Qatu, M.S. (2012), "Statics and vibration analyses of thick deep laminated cylindrical shells using 3D and various shear deformation theories", *Compos. Struct.*, **94,** 494-500. https://doi.org/10.1016/j.compstruct.2011.08.011

Chan, D.Q., Nguyen, P.D., Quang, V.D., Anh, V.T.T. and Nguyen, D.D. (2019), "Nonlinear buckling and post-buckling of functionally graded CNTs reinforced composite truncated conical shells subjected to axial load", *Steel Compos. Struct., Int. J.*, **31**(3), 243-259. https://doi.org/10.12989/scs.2019.31.3.243

Chang, T. and Gao, H. (2003), "Size-dependent elastic properties of a single-walled carbon nanotube via a molecular mechanics model", *J. Mech. Phys. Solids*, **51**, 1059-1074. https://doi.org/10.1016/S0022-5096(03)00006-1

Chavan, G.S. and Lal, A. (2017), "Bending behavior of SWCNT reinforced composite plates", *Steel Compos. Struct., Int. J.*, **24**(5), 537-548. https://doi.org/10.12989/scs.2017.24.5.537

Ebrahimi, F. and Habibi, S. (2017), "low-velocity impact response of laminated FG-CNT reinforced composite plates in thermal environment", *Adv. Nano Res., Int. J.*, **5**(2), 69-97. https://doi.org/10.12989/anr.2017.5.2.069

Emdadi, M., Mohemmadimehr, M. and Navi, B.R. (2019), "Free vibration of an annular sandwich plate with CNTRC face sheets and FG porous cores using Ritz method", *Adv. Nano Res., Int. J.*, **7**(2), 109-123. https://doi.org/10.12989/anr.2019.7.2.109

Fu, T., Chen, Z., Yu, H., Wang, Z. and Liu, X. (2019), "Mechanical behavior of laminated functionally graded carbon nanotube-reinforced composite plates resting on elastic foundations in thermal environments", *J. Compos. Mater.*, **53**(9), 1159-1179. https://doi.org/10.1177/002F0021998318796170

Hajmohammad, M.H., Zarei, M.S, Farrokhian, A. and Kolahchi, R. (2018), "A layerwise theory for buckling analysis of truncated conical shells reinforced by CNTs and carbon fibers integrated with piezoelectric layers in hygrothermal environment", *Adv. Nano Res., Int. J.*, **6**(4), 299-321. https://doi.org/10.12989/anr.2018.6.4.299

Hajnayeb, A. and Khadem, S.E. (2015), "An analytical study on the nonlinear vibration of a double walled carbon nanotube", *Struct. Eng. Mech., Int. J.*, **54**(5), 987-998. https://doi.org/10.12989/sem.2015.54.5.987

Hussain, M., Naeem, M.N., Tounesi, A. and Taj, M. (2019), "Nonlocal effect on the vibration of armchair and zigzag SWCNTs with bending rigidity", *Adv. Nano Res., Int. J.*, **7**(6), 431-432. https://doi.org/10.1989/anr. 2019.7.6.431

Jedari Salami, S. (2016a), "Extended high order sandwich panel theory for bending analysis of sandwich beams with carbon nanotube reinforced face sheets", *Physica E*, **76**, 187-197. https://doi.org/10.1016/j.physe.2015.10.015

Jedari Salami, S. (2016b), "Dynamic extended high order sandwich panel theory for transient response of sandwich beams with carbon nanotube reinforced face sheets", *Aerosp. Sci. Technol.*, **56**, 56-69. https://doi.org/10.1016/j.ast.2016.06.026

Jedari Salami, S. (2017), "Low velocity impact response of sandwich beams with soft cores and carbon nanotube reinforced face sheets based on extended high order sandwich panel theory", *Aerosp. Sci. Technol.*, **66**, 165-176. https://doi.org/10.1016/j.ast.2017.03.007

Jedari Salami, S. (2018), "Free vibration analysis of sandwich beams with carbon nanotube reinforced face sheets based on extended high-order sandwich panel theory", *J. Sandw. Struct. Mater.*, **20**(2), 219-248. https://doi.org/10.1177/1099636216649788

Jamali, M., Shojaee, T., Mohammadi, B. and Kolahchi, R. (2019), "Cut out effect on nonlinear post-buckling behavior of FG-CNTRC microplate subjected to magnetic field via FSDT", *Adv. Nano Res., Int. J.*, **7**(6), 405-417. https://doi.org/10.12989/anr.2019.7.6.405

Kamarian, S., Shakeri, M., Yas, M.H., Bodaghi, M. and Pourasghar, A. (2015), "Free vibration analysis of functionally graded nanocomposite sandwich beams resting on Pasternak foundation by considering the agglomeration effect of CNTs", *J. Sandw. Struct. Mater.*, **17**(6), 632-665. https://doi.org/10.1177/1099636215590280

Kamarian, S., Bodaghi, M., Pourasghar, A. and Talebi, S. (2016), "Vibrational Behavior of Non-Uniform Piezoelectric Sandwich Beams Made of CNT-Reinforced Polymer Nanocomposite by Considering the Agglomeration Effect of CNTs", *Polym. Compos.*, **38**(S1), 553-562. https://doi.org/10.1002/pc.23933

Kamarian, S., Bodaghi, M., Barbaz Isfahani, R., Shakeri M. and Yas, M.H. (2019), "Influence of carbon nanotubes on thermal expansion coefficient and thermal buckling of polymer composite plates: experimental and numerical investigations", *Mech. Based Des. Struct. Machines*, **49**(2), 217-2322. https://doi.org/10.1080/15397734.2019.1674664

Karami, B., Shahsavari, D. and Janghorban, M. (2018), "A comprehensive analytical study on functionally graded carbon nanotube-reinforced composite plates", *Aerosp. Sci. Technol.*, **82-83**, 499-512. https://doi.org/10.1016/j.ast.2018.10.001

Karimov, K.S., Nabi, J.-U., Ali, R., Fatima, N., Khan, A., Rehman, M.M. and Bashir, M.M. (2020), "Resistive and impedimetric properties of elastic composite based on graphene and CNT under uniaxial compressive displacement", *Adv. Compos. Mater.*, **29**(6), 559-568. https://doi.org/10.1080/09243046.2020.1731104

Khater, H.M. and Abd El Gawwad, H.A. (2015), "Effect of firing temperatures on alkali activated Geopolymer mortar doped with MWCNT ", *Adv. Nano Res., Int. J.*, **1**(2), 225-242. https://doi.org/10.12989/anr. 2015.3.4.225

Kumar, D. and Sirvastava, A. (2016), "Elastic properties of cnt- and graphene-reinforced nanocomposites using RVE", *Steel Compos. Struct., Int. J.*, **21**(5), 1085-1103. https://doi.org/10.12989/scs.2016.21.5.1085

Lei, Z.X., Liew, K.M. and Yu, J.L. (2013), "Free vibration analysis

of functionally graded carbon nanotube-reinforced composite plates using the element-free kp-Ritz method in thermal environment", *Compos*. *Struct*., **106**, 128-138. https://doi.org/10.1016/j.compstruct.2013.06.003

Liew, K.M., Lei, Z.X. and Zhang, L.W. (2015), "Mechanical analysis of functionally graded carbon nanotube reinforced composites: a review", *Compos*. *Struct*., **120**, 90-97. https://doi.org/10.1016/j.compstruct.2014.09.041

Mirzaei, M. and Kiani, Y. (2015), "Thermal buckling of temperature dependent FG-CNT reinforced composite conical shells", *Aerosp*. *Sci*. *Technol*., **47**, 42-53. https://doi.org/10.1016/j.ast.2015.09.011

Navneeth, V., Sankar, S.P., Prasanth, R.S. and Samsingh, R.V. (2020), "Investigation on the mechanical and stealth behavior of CNT based polymer composites", *Mater*. *Today*: *Proceedings*, **39**, 1682-1687. https://doi.org/10.1016/j.matpr.2020.06.152

Shen, H. (2009), "Nonlinear bending of functionally graded carbon nanotube reinforced composite plates in thermal environments", *Compos*. *Struct*., **91**(1), 9-19. https://doi.org/10.1016/j.compstruct.2009.04.026

Shen, H. (2012), "Thermal buckling and postbuckling behavior of functionally graded carbon nanotube-reinforced composite cylindrical shells", *Compos*. *Part B*: *Eng*., **43**, 1030-1038. https://doi.org/10.1016/j.compositesb.2011.10.004

Shen, H. and Xiang, Y. (2014), "Nonlinear bending of nanotube-reinforced composite cylindrical panels resting on elastic foundations in thermal environments", *Eng*. *Struct*., **80**, 163-172. https://doi.org/10.1016/j.engstruct.2014.08.038

Song, Y.S. and Youn, J.R. (2006), "Modeling of effective elastic properties for polymer-based carbon nanotube composites", *Polymer*, **47**, 1741-1748. https://doi.org/10.1016/j.polymer.2006.01.013

Wang, Z.X. and Shen, H.S. (2011), "Nonlinear vibration of nanotube-reinforced composite plates in thermal environments", *Comput*. *Mater*. *Sci*., **50**, 2319-2330. https://doi.org/10.1016/j.commatsci.2011.03.005

Wang, Z.X. and Shen, H.S. (2012), "Nonlinear vibration and bending of sandwich plates with nanotube-reinforced composite face sheets", *Composites*: *B*, **43**, 411-421. https://doi.org/10.1016/j.compositesb.2011.04.040

Zhang, L., Lei, Z.X., Liew, K.M. and Yu, J.L. (2014), "Static and dynamic of carbon nanotube reinforced functionally graded cylindrical panels", *Compos*. *Struct*., **111**(1), 205-212. https://doi.org/10.1016/j.compstruct.2013.12.035

Zhang, L., Lei, Z.X. and Liew, K.M. (2015a), "Free vibration analysis of functionally graded carbon nanotube-reinforced composite triangular plates using the FSDT and element-free IMLS-Ritz method", *Compos*. *Struct*., **120**(1), 189-199. https://doi.org/10.1016/j.compstruct.2014.10.009

Zhang, L., Lei, Z.X. and Liew, K.M. (2015b), "Vibration characteristic of moderately thick functionally graded carbon nanotube reinforced composite skew plates", *Compos*. *Struct*., **122**(1), 172-183. https://doi.org/10.1016/j.compstruct.2014.11.070

Zhao, X. and Liew, K.M. (2009), "Geometrically nonlinear analysis of functionally graded shells", *Int*. *J*. *Mech*. *Sci*., **51**(2), 131-144. https://doi.org/10.1016/j.ijmecsci.2008.12.004

Appendix

$$(K_T)_{ij} = \frac{\partial R_i}{\partial U_{lm}}, \quad for\ 1 \le j \le N_x N_y \ \rightarrow$$
$$J = j \rightarrow\ l = \left[\frac{J-1}{N_y}\right] + 1, \quad m = j - N_y \left[\frac{J-1}{N_y}\right]$$

$$(K_T)_{ij} = \frac{\partial R_i}{\partial V_{lm}}, \quad for \quad N_x N_y + 1 \le j \le 2N_x N_y \ \rightarrow$$
$$J = j - N_x N_y \rightarrow l = \left[\frac{J-1}{N_y}\right] + 1, \quad \mathrm{m} = j - N_y \left[\frac{J-1}{N_y}\right]$$

$$(K_T)_{ij} = \frac{\partial R_i}{\partial W_{lm}}, \quad for \quad 2N_x N_y + 1 \le j \le 3N_x N_y \ \rightarrow$$
$$J = j - 2N_x N_y\ l = \left[\frac{J-1}{N_y}\right] + 1, \quad m = j - N_y \left[\frac{J-1}{N_y}\right]$$

$$(K_T)_{ij} = \frac{\partial R_i}{\partial X_{lm}}, \quad for \quad 3N_x N_y + 1 \le j \le 4N_x N_y \ \rightarrow$$
$$J = j - 3N_x N_y \rightarrow l = \left[\frac{J-1}{N_y}\right] + 1, \quad m = j - N_y \left[\frac{J-1}{N_y}\right]$$